European methodology for testing the airborne sound insulation characteristics of noise barriers *in situ*: Experimental verification and comparison with laboratory data

Massimo Garai[a] and Paolo Guidorzi
Department of Energetic, Nuclear and Environmental Control Engineering (DIENCA), Università di Bologna, Viale Risorgimento, 2, 40136 Bologna, Italy

(Received 3 December 1999; accepted for publication 9 May 2000)

In the frame of the 1994–1997 *Standard, Measurement and Testing* program, the European Commission funded a research project, named *Adrienne*, to define new test methods for measuring the intrinsic characteristics of road traffic noise reducing devices *in situ*. The research team produced innovative methods for testing the sound reflection/absorption and the airborne sound insulation characteristics of noise barriers. These methods are now under consideration at CEN (European Committee for Standardization), to become European standards. The present work reports a detailed verification of the test method for airborne sound insulation over a selection of 17 noise barriers, representative of the Italian and European production. The samples were tested both outdoors, using the new *Adrienne* method, and in laboratory, following the European standard EN 1793-2. In both cases the single number rating for airborne sound insulation recommended by the European standard was calculated. The new method proved to be easy to use and reliable for all kinds of barriers. It has been found sensitive to quality of mounting, presence of seals, and other details typical of outdoor installations. The comparison between field and laboratory results shows a good correlation, while existing differences can be explained with the different sound fields and mounting conditions between the outdoor and laboratory tests. It is concluded that the *Adrienne* method is adequate for its intended use.
[S0001-4966(00)03208-2]

PACS numbers: 43.50.Gf, 43.50.Sr, 43.50.Lj [MRS]

INTRODUCTION

The role of noise barriers in reducing the impact of road and train noise is widely acknowledged by the international community.[1] The effectiveness of noise barriers depends on several factors such as

(i) barrier geometry: height, length, thickness, shape;
(ii) barrier acoustical characteristics: sound reflection and diffusion of the surface exposed to noise, airborne sound insulation;
(iii) installation-related factors: quality of workmanship, way of mounting (panel–post and panel–panel assembling mechanism), presence of seals;
(iv) deterioration with time;
(v) site geometry: ground profile, screen position relative to noise sources and receivers;
(vi) site acoustical characteristics: ground impendance; and
(vii) meteorological conditions: wind, temperature gradients, etc.

Among these, airborne sound insulation is important to attenuate the noise transmitted directly through the screen so that it is not significant compared with the sound diffracted over the top edge. Airborne sound insulation of installed screens depends on two classes of factors:

(i) intrinsic characteristics: airborne sound insulation, quality of workmanship, way of mounting, presence of seals; and
(ii) extrinsic characteristics: all the other site-related characteristics.

Only the intrinsic characteristics are relevant to qualify the product itself. Therefore, a method should be available to test on the installation site the compliance of the intrinsic characteristics of the installed product to the design specifications. Moreover, installed noise barriers may change their characteristics with time; therefore, existing noise barriers should be regularly tested *in situ*, i.e., along roads and railways where they are installed, to check the possible decay of their acoustical properties.

For all these reasons, there is a strong need of a method to test the intrinsic characteristics of noise barriers *in situ*. On the other hand, no such method exists at international level. In most European countries only laboratory tests are performed, accordingly with the new EN 1793-1, 1793-2, and 1793-3[2–4] (European standards are identified by the two letters EN before their number). The European standards rely on the ISO 354[5] for sound absorption and the ISO 140-3[6] for airborne sound insulation, with the additional requirement that a post must be included in the laboratory specimen (when applicable for the specific kind of barrier). The abovementioned ISO standards have been designed for building products and therefore require the tests to be performed inside special rooms under a diffuse sound field, which is very

[a]Electronic mail: massimo.garai@mail.ing.unibo.it

different from the sound field in front of an installed noise barrier. As a result, the airborne sound insulation of noise barriers in their intended use is underestimated.[7] Furthermore, the most common defects of actual installations along roads and railways, like sound leakage due to poor workmanship, bad connections between panels and posts, absence of seals, etc., cannot be detected using laboratory methods.

At national level, there is only one standard regarding *in situ* measurements, used in France.[8] However, this method relies on the use of a gunshot as sound source, which has a poor repeatability, and a short time window for the analysis (3 ms in length), which limits the lowest reliable frequency to the one-third octave band of 400 Hz. Moreover, the placement of the analysis window is left to the operator's choice. For these reasons, the French method has not been accepted by the European Committee for Standardization (CEN).[7,9,10]

Recognizing that this situation is an obstacle to the free circulation of noise barriers on the European market, the European Commission, in the frame of the 1994–1997 *Standard, Measurement and Testing* (SMT) program, funded a research project, named *Adrienne*, to define new test methods for measuring the intrinsic characteristics of road traffic noise reducing devices *in situ*. After a three-year work, the research team produced innovative methods for testing the sound reflection/absorption and the airborne sound insulation characteristics of noise barriers. These methods are now under consideration at CEN, in CEN/TC 226/WG6 (Technical Committee 226, Working Group 6), to become European standards. The present work reports a detailed verification of the *Adrienne* airborne sound insulation test method on a selection of 17 noise barriers, representative of the Italian and European market. The samples were tested both outdoors, using the new *Adrienne* method in controlled conditions, and in laboratory, following the EN 1793-2 standard. In both cases the single number rating for airborne sound insulation recommended by the European standard was calculated.[3] The main aims of the work were at least three:

(i) to test the practicability and the reliability of the new *Adrienne* method for different kinds of barriers (composed mainly of concrete, metal, acrylic or wood; having a flat or nonflat surface; having an absorbing or reflecting surface; etc.);
(ii) to test the sensitivity of the new method to quality of workmanship, way of mounting, and other details typical of real outdoor installations; these sources of possible problems are present in real situations but are carefully eliminated when preparing laboratory specimens; and
(iii) to compare the outdoor and laboratory airborne sound insulation values obtained on the same set of barrier samples and to investigate their possible correlation, which would be useful for predicting the expected field performance from laboratory data.

I. THE SAMPLES

All samples had the same global size: about $3.0 \times 3.5\,m^2$ for the laboratory test (the size of the test opening between the coupled rooms) and $18.0 \times 4.0\,m^2$ for the outdoor test. The basic characteristics of the 17 barrier samples are summarized in Table I. The barrier samples are presented with conventional names in order to not disclose the producer names. The barriers submitted to the test can be grouped in six classes:

(1) Concrete barriers (five samples): a typical barrier element is made of a heavy concrete back panel supporting a front panel made with lighter concrete and with a nonflat shape, in order to increase the sound absorption of the surface. The posts are large and strong to support the considerable weight of the structure.
(2) Metallic barriers (seven samples): a typical barrier element is a box made with a metallic sheet having a thickness ranging from 1 to 2 mm. The box is perforated on one face and partially filled with a high-density rock wool. In two cases a high-density synthetic damper was added (MET2 and MET7). In two cases the metallic sheet was not folded to form a box and not perforated (MET4 and MET5). The posts are metallic beams with a ''*H*'' section and 160 mm wide.
(3) Resin barriers (one sample): the barrier elements are boxes made with a 3-mm-thick polyether resin sheet reinforced using glass fibers. The boxes are perforated on one face and partially filled with a glass fiber blanket. The posts, 100 mm wide, are made of the same polyether resin, using a layer 10 mm thick.
(4) Acrylic barriers (one sample): the barrier elements are transparent polymethylmethacrylate (PMMA) sheets, 20 mm thick, supported by a light metallic frame.
(5) Mixed barriers (one sample): the half-barrier close to the ground is made of metallic panels, like those described above (point 2); the upper half is made of transparent polymethylmethacrylate (PMMA) sheets, 15 mm thick, supported by a light metallic frame. The posts are metallic beams with a ''*H*'' section and 160 mm wide.
(6) Wood barriers (one sample): the barrier is made of four layers i.e., from front to back, wood tiles made of spaced laths; rock wool blanket; fiber–concrete aggregate board; wood board. The posts are metallic beams with a ''*H*'' section and 160 mm wide.

II. LABORATORY MEASUREMENTS

The laboratory test method specified in EN 1793-2[3] fully conforms to the well-known ISO 140-3,[6] with some additions particularly relevant for noise barriers. The most important points of the procedure are summarized in the following.

The measurements are performed in laboratory test facilities consisting of two adjacent reverberant rooms, called the source room and the receiving room, respectively, with an opening between them in which the test specimen is inserted. Transmission of sound on flanking paths must be suppressed. The measurements reported in the present work were performed in a laboratory where the test aperture is about $3.0 \times 3.5\,m^2$ (width×height). When necessary, a filler wall with a significantly better sound insulation than the test specimen was used to fit the specimen in the aperture.

Following EN 1793-2, the test specimen must be mounted in the test opening and assembled in the same man-

TABLE I. Basic characteristics of the tested barriers.

Sample	Type	Basic elements composition	Element thickness (mm)	Element height (m)	Element width (m)
CON1	Concrete	Back: concrete 2500 kg/m^3 Front: light clay aggregate 1250 kg/m^3	275	2.00	4.50
CON2	Concrete	Back: concrete 2500 kg/m^3 Front: light clay aggregate 1250 kg/m^3	250	2.00	3.00
CON3	Concrete	Back: concrete 2500 kg/m^3 Front: light clay aggregate 1250 kg/m^3	250	2.00	3.00
CON4	Concrete	Back: concrete 2050 kg/m^3 Front: light clay aggregate blocks (1000 kg/m^3) with holes (resonators)	220	2.00	3.26 (last: 1.70)
CON5	Concrete	Back: concrete 2500 kg/m^3 Front: light clay aggregate 1200 kg/m^3	190	4.00	2.40 (last: 1.20)
CON6	Concrete	Back panel: concrete 2500 kg/m^3 Front panel: grooved light concrete	240	1.00	4.00 (last: 2.00)
MET1	Metal	Box made with a 1.5-mm metallic sheet, perforated on one face and filled with a 100-kg/m^3 rock wool blanket, 80 mm thick	119	0.50	4.00 (last: 2.00)
MET2	Metal	Curved box made with a 1.5-mm metallic sheet, perforated on one face and filled with an 85-kg/m^3 rock wool blanket, 50 mm thick, and a high-density synthetic damper	130	0.50	4.00 and 3.00
MET3	Metal	Box made with a 1.5-mm metallic sheet, perforated on one face and filled with a 95-kg/m^3 rock wool blanket, 60 mm thick	115	0.50	3.00
MET4	Metal	Single 1.0-mm metallic sheet, folded to form protruding supports 60 mm wide	60	0.50	4.00 (last: 2.00)
MET5	Metal	Single 1.0-mm metallic sheet, folded to form protruding supports, 60 mm wide, containing panels in polyesther fibre wool, thickness 50 mm, density 50 kg/m^3. Frontal protection grid.	60	0.50	4.00 (last: 2.00)
MET6	Metal	Box made with a 1.0-mm metallic sheet, perforated on one face and filled with a 100-kg/m^3 rock wool blanket, 40 mm thick	122	0.50	3.00
MET7	Metal	Box made with a 1.8-mm metallic sheet, perforated on one face and filled with a 85-kg/m^3 rock wool blanket, 40 mm thick, and a high-density synthetic damper	80	0.50	4.00 and 3.00
RES1	Resin	Box made with a 3-mm-thick polyether resin sheet reinforced using glass fibers, perforated on one face and filled with a 60-kg/m^3 glass fiber blanket, 40 mm thick	86	0.50	3.00
ACR1	Acrylic	Polymethylmethacrylate (PMMA) sheets 20 mm thick, supported by a metallic frame, 130 mm thick	20	2.00	3.00
MIX1	Bottom (0 to 2 m): metal; top (2 to 4 m): acrylic	Box made with a 1.5-mm metallic sheet, perforated on one face and filled with a 90-kg/m^3 rock wool blanket, 60 mm thick. Polymethyl methacrylate (PMMA) sheets 15 mm thick, supported by a metallic frame, 120 mm thick	120/15	0.50/2.00	3.00
WOOD	Wood	From front to back: wood tiles 1×1 m^2, made of spaced laths 19 mm thick; 90-kg/m^3 rock wool blanket, 60 mm thick; fiber-concrete aggregate board, 4 mm thick; wood board, 19 mm thick	127	1.00	3.00

ner as the manufactured device used in practice, with the same connections and seals between component parts. The edge supports must not overlap the sample by more than 70 mm and must be sealed to prevent leakage of sound. Where posts are employed in construction, at least one post must be included in the specimen, with panels attached on both sides. The length of the panels on one side of the post must be greater than or equal to 2 m. The side that would face the traffic noise source must face the source room.

In the source room a loudspeaker produces a continuous

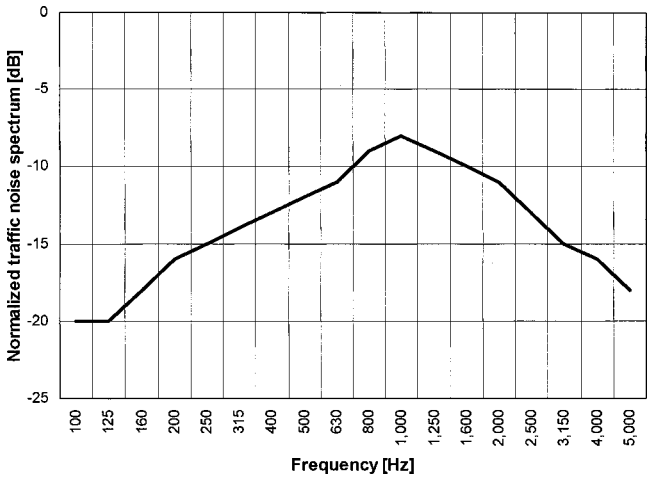

FIG. 1. Normalized A-weighted traffic noise spectrum from EN 1793-3.

broadband noise (pink noise was used in the present work) in the one-third octave bands from 100 Hz to 5 kHz. Moving microphones are used to obtain the average sound pressure levels in each room. Measurements are repeated moving the loudspeaker in different positions and averaged. The values of the airborne sound reduction index R_j, in each frequency band, is then calculated from the equation

$$R_j = L_{p,1,j} - L_{\rho,2,j} + 10 \cdot 1g \frac{S}{A_j} (\mathrm{dB}), \tag{1}$$

where j is the index of the one-third octave bands from 100 Hz to 5 kHz; $L_{p,1,j}$ is the average sound pressure level in the source room (dB); $L_{p,2,j}$ is the average sound pressure level in the receiving room (dB); S is the area of the test specimen (m^2); and A_j is the equivalent absorption area in the receiving room (m^2).

The sound generation chain was assembled with a WR-Electronics loudspeaker, a Masters PWA-202/4 power amplifier, a Brüel & Kjær type 1405 noise generator, and an Applied Research & Technology, Inc. HD-31 equalizer. The sound field was sampled using two microphones, Brüel & Kjær type 4192, with pre-amplifiers, Brüel & Kjær type 2669, connected to a Brüel & Kjær analyzer (a type 2144 and a type 2123 were used).

According to EN 1793-2, a single number rating of sound insulation, DL_R, must be calculated to give an overall indication of the performance of the product. It is defined as

$$DL_R = -10 \lg \left[\frac{\Sigma_{j=1}^{18} 10^{0.1 L_j} 10^{-0.1 R_j}}{\Sigma_{j=1}^{18} 10^{0.1 L_j}} \right] (\mathrm{dB}), \tag{2}$$

where L_j is the normalized A-weighted sound pressure level of traffic noise in the jth one-third octave band (dB), as defined in EN 1793-3,[4] (see Fig. 1). DL_R must be given rounded to the nearest integer. If there is a need to categorize airborne sound insulation, this is done on the basis of the DL_R value, using the categories listed in Table II. It is worth noting that the normalized traffic noise spectrum comes from the average of road traffic noise spectra taken in Europe; consequently, greatest weight is given to performance at frequencies that are important in European road traffic noise. It is also worth noting that DL_R is different, for the calculation procedure and the reference spectrum, from the well-known rating R_w used in building acoustics.[11]

TABLE II. Categories of airborne sound insulation (EN 1793-2).

Category	DL_R (dB)
B0	Not determined
B1	<15
B2	15 to 24
B3	>24

Examples of measured values of the sound reduction index, R_j, in the one-third octave frequency bands from 100 Hz to 5 kHz, are reported in graphical form in Figs. 10–17 together with the corresponding outdoor measurement results (see Sec. IV). All values of the ratings R_w and DL_R are reported in Table III. The DL_R values were calculated both on the full frequency range 100 Hz to 5 kHz, in one-third octave frequency bands, and in the ''restricted'' frequency range 200 Hz to 5 kHz; the latter calculation was made in view of the comparison with the single number rating values resulting from the outdoor measurements, which have a low-frequency limit of about 160 Hz and then a valid frequency range going from 200 Hz to 5 kHz, in one-third octave frequency bands (see Sec. IV C).

III. SUMMARY OF THE *ADRIENNE* TEST METHOD FOR AIRBORNE SOUND INSULATION

As the *Adrienne* test method is rather new, it will be summarized here in more detail than the laboratory method. However, this summary is not intended to explain the reason of each choice made during the development of the *Adrienne* research; for this, reference should be made to Refs. 7 and 10.

A. Review of previous literature

The *Adrienne* method is based on the recovering of an acoustic impulse response behind the barrier under test; to this extent it has an ideal connection with transient methods proposed for testing the transmission loss of partitions in buildings. The first attempt was made by Raes,[12] who used sinusoidal waves with exponential modulated amplitude as test signal and compared the maximum amplitude of the incident and transmitted sound signals in the time domain. In a subsequent paper, Raes[13] distinguished between ''static'' and ''dynamic'' transmission loss, the first being measured using a stationary sound field, the latter using an impulsive excitation. He pointed out that measuring the transmission loss using transient sound signals is closer to real life situations, where most noise sources are not stationary and do not produce a diffuse sound field. De Tricaud,[14] using a pistol shot as sound source, obtained a fairly good agreement between impulsive and classical measurements of transmission loss in buildings. He remarked that the pistol shot should have the same power spectrum of the loudspeaker used in the conventional method (at least in octave bands) for the results of the two tests be comparable. He also claimed that impulsive methods are more robust against extraneous noise. Roland[15] improved the de Tricaud technique, pointing out

TABLE III. Single number ratings of airborne sound insulation.

Sample	Type	R_w (dB) laboratory 100 Hz to 5 kHz	DL_R (dB) laboratory 100 Hz to 5 kHz	DL_R (dB) laboratory 200 Hz to 5 kHz	DL_{SI} (dB) outdoors elements 200 Hz to 5 kHz	DL_{SI} (dB) outdoors posts 200 Hz to 5 kHz
CON1	Concrete	56	52	54	63	61
CON2(Q)	Concrete	46	44	44	57	38
CON2(A)	Concrete	56	52	53	57	38
CON3	Concrete	53	48	50	62	54
CON4	Concrete	55	50	51	60	64
CON5	Concrete	48	45	45	55	57
CON6	Concrete	53	50	51	59	55
MET1	Metal	36	31	33	39	33
MET2	Metal	33	29	31	32	35
MET3	Metal	36	31	34	37	33
MET4	Metal	26	23	23	31	26
MET5	Metal	30	26	26	32	32
MET6	Metal	34	28	31	30	34
MET7	Metal	30	28	28	33	36
RES1	Resin	27	23	25	25	23
ACR1	Acrylic	36	33	33	40	40
MIX1	Metal/acrylic	32	30	31	37	29
WOOD	Wood	34	30	30	34	27

that, for best comparability of the classical and transient methods, (i) the source used to emit the test signal should be the same in both cases or, at least, should have the same acoustical characteristics (directivity, volume, etc.) and (ii) peaks in the transient test signal should be not so high as to violate the linear acoustic assumptions. Davies and Gibbs[16] applied the impulse method to a freely suspended Perspex panel. They refined the measurement technique using a digitally generated pulse (square wave), inverted each two cycles and synchronously averaged 256 times. This test signal is much closer to a maximum length sequence (MLS) than to a pistol shot. Balilah and Gibbs,[17] continuing the work of Davies and Gibbs with a better instrumentation, tested different samples, in laboratory and *in situ*. Systematic computations of time of flights permitted the identification of the sound radiation due to bending wave propagation in the plates under test. Zuomin and Chu[18] proved that transmission loss measurements can be made in the laboratory using a MLS signal. They also provided an empirical formula to estimate the number of averages required to reach a desired accuracy in the presence of a given signal-to-noise ratio. All the above-mentioned authors were mainly concerned with building acoustics measurements; no tests were performed on noise barriers installed outdoors.

B. General principle

A loudspeaker is placed facing the traffic side of the barrier under test, a microphone is placed on the opposite side. The loudspeaker emits a test sound wave that is partly reflected, partly transmitted, and partly diffracted by the noise barrier (see Fig. 2). The microphone receives a signal that, suitably postprocessed, gives an overall impulse response. This includes the transmitted component, traveling from the sound source through the noise barrier to the microphone; the component diffracted by the top edge of the screen; and other ''parasitic'' components (reflected from the ground, both on the source and the receiver side; diffracted from the lateral edges, etc.). In particular, for the test to be meaningful, the diffraction from the lateral edges should be sufficiently weak and delayed. The transmitted sound pressure wave can be extracted by the global impulse response applying a suitable time window. If the measurement is repeated without the noise barrier between the loudspeaker and

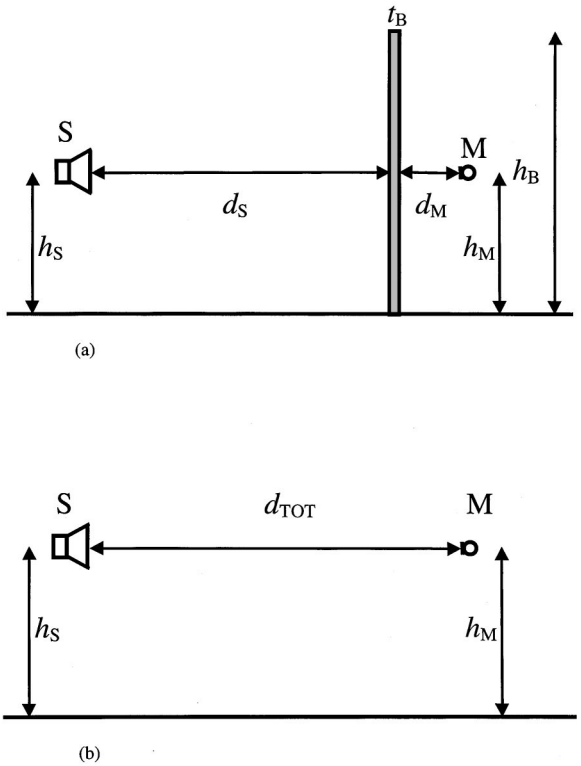

FIG. 2. Sketch of the setup for the sound insulation index measurement. Normal sound incidence of sound on the sample. S: loudspeaker. M: microphone. (a) Transmitted sound measurement. (b) Free-field (incident) sound measurement.

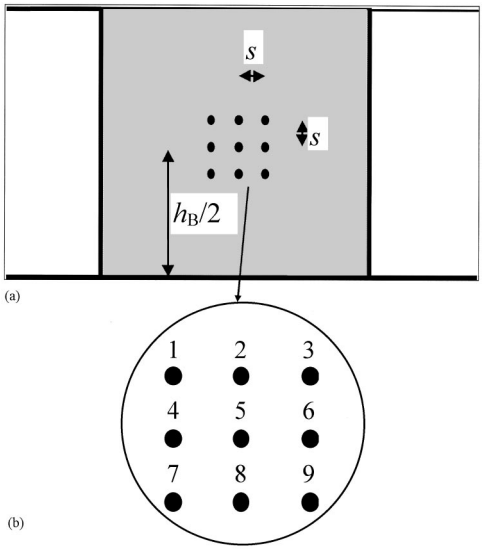

FIG. 3. (a) Grid of the microphone positions for the measurement by scanning at discrete points on a test section of a noise barrier (front view, receiver side). (b) Numbering of the measurement points.

the microphone (this is called ''free-field'' measurement in Ref. 7), the direct component alone can be sampled. The power spectra of the direct ''free-field'' component and the transmitted component, corrected to take into account the path length difference of the two signals, gives the basis for calculating the outdoor transmission loss [see Eq. (3)], which has been called *sound insulation index*.[10]

The measurement in front of the barrier is repeated at nine points placed on an ideal grid (scanning points). The final sound insulation index is the logarithmic average of the results in these nine positions (see Fig. 3).

C. Measured quantity

The expression used to compute the *sound insulation index SI* as a function of frequency is[7,10]

$$\mathrm{SI}_j = -10\,\lg\left\{\frac{\Sigma_{k=1}^{n}\int_{\Delta f_j}\left|\mathbf{F}[p_{tk}(t)w_{tk}(t)]\right|^2 df (d_k/d_i)^2}{n\cdot\int_{\Delta f_j}\left|\mathbf{F}[p_i(t)w_i(t)]\right|^2 df}\right\}\ (\mathrm{dB}), \tag{3}$$

where $p_i(t)$ is the reference free-field component; $p_{tk}(t)$ is the transmitted component at the kth scanning point; d_i is the geometrical spreading correction factor for the reference free-field component; d_k is the geometrical spreading correction factor for the transmitted component at the kth scanning point ($k=1,...,n$); $w_i(t)$ is the time window (*Adrienne* window) for the reference free-field component; $w_{t,k}(t)$ is the time window (*Adrienne* window) for the transmitted component at the kth scanning point; **F** is the symbol of the Fourier transform; Δf_j is the jth one-third octave frequency band (from 100 Hz to 5 kHz); and $n=9$ is the number of scanning points.

The geometrical spreading correction factors d_i (incident wave) and d_k ($k=1,...,9$) are (see Figs. 2 and 3)

$$d_i = d_5 = d_{SM} = d_s + t_B + d_M = 1{,}25 + t_B, \tag{4}$$

$$d_2 = d_4 = d_6 = d_8 = \sqrt{d_i^2 + s^2}, \tag{5}$$

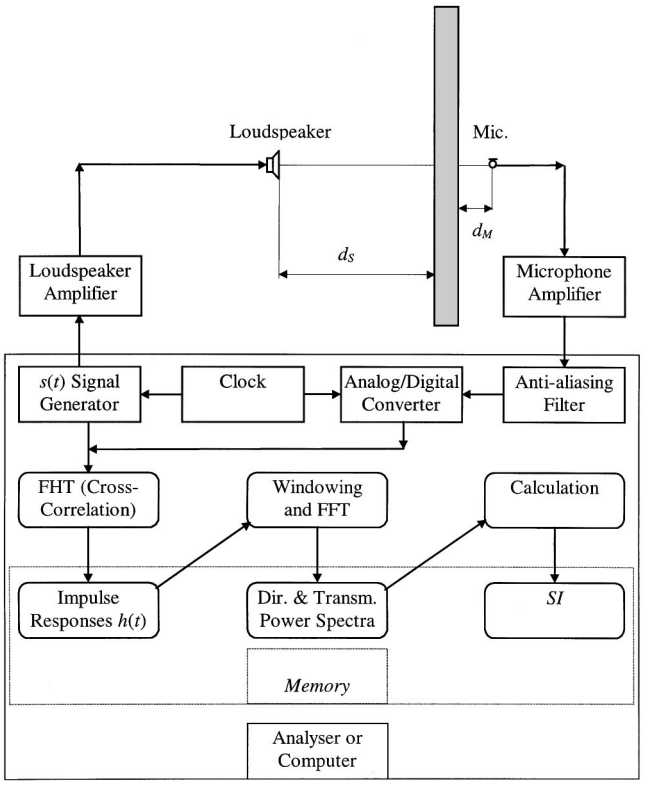

FIG. 4. Sketch representing the essential components of the measuring system.

$$d_1 = d_3 = d_7 = d_9 = \sqrt{d_i^2 + 2s^2}, \tag{6}$$

where t_B is the barrier thickness (m) and s is the measurement grid step (m) (see Fig. 3).

The frequency domain integration in Eq. (3) indicates the reconstruction of the one-third octave band values SI_j from narrow-band data. The European standards require results be presented in the one-third octave bands from 100 Hz to 5 kHz.

D. Measuring equipment and procedure

1. Measuring system

The measuring equipment comprises an electro-acoustical source, consisting of an electrical signal generator, a power amplifier and a loudspeaker; a microphone with its microphone amplifier; and a signal analyzer capable of performing transformations between the time domain and the frequency domain. Part of these devices can be integrated into a frequency analyzer or a personal computer equipped with specific add-on board(s). The essential components of the measuring system are shown in Fig. 4.

The impulse response is acquired using the well-known MLS technique[19–22] that allows the measurement be done without impulse excitation. A MLS is a deterministic sequence of bipolar pulses. Its frequency spectrum is white and its circular autocorrelation function is approximately a periodic unit-sample, with a negligible dc component. The loudspeaker, driven with an input electrical signal consisting of a MLS, excites the device under test (Fig. 4). The system impulse response is derived from the signal picked up by the microphone applying a fast Hadamard transform (FHT). This

is equivalent to cross correlating the microphone signal with the MLS fed to the loudspeaker.[20,21,23] The sample rate of the acquisition device must be equal to the clock rate of the MLS signal generator. The MLS technique is highly noise rejecting compared to more conventional ones;[21,24] the signal-to-noise ratio can be further improved by synchronous averaging.[25] An important prerequisite of the MLS technique is that the system under test must be linear and time invariant (LTI system).

An absolute calibration of the measurement chain with regard to the sound pressure level is not needed, because the measurement procedure described here is based on the ratio of the power spectra of signals extracted from impulse responses sampled with the same equipment in the same place under the same conditions.

For the *Adrienne* test method, the sample rate f_s must have a value greater than 43 kHz.[7] Although the signal is already unambiguously defined when the Nyquist criterion is met, higher sample rates facilitate a clear reproduction of the signal. Errors can be detected and corrected more easily, such as corrections needed to account for time shifts due to temperature changes. It is worth noting that *Adrienne* requirements are the same for sound insulation index and sound reflection index measurements. The *sound reflection index* is the quantity introduced to characterize the reflecting and diffusing property of noise barriers (not treated in the present article).[7,10] The *sound reflection index* is calculated using the signal subtraction technique,[26] which necessitates of an exact reproduction of time signals and therefore of high sample rate values.

2. Positioning of the measuring equipment

The measuring equipment must be placed near the noise reducing device to be tested according to the following rules.

A *source reference plane* is defined as the vertical plane tangential to the most protruding edges of the sample, on the traffic side. A *reference position* is located on this reference plane at a height equal to half the height h_B of the barrier under test. The loudspeaker is placed in front of the reference position at a horizontal distance d_S of 1 m from the source reference plane and at a height h_S equal to half the barrier height [Fig. 2(a)].

On the opposite side of the barrier under test *a microphone reference plane* is located and an *ideal measurement grid* is defined on it. The measurement grid must be squared, with a side length of 0.80 m. The measurement grid shall be at a distance d_M of 0.25 m from the plane of reference for the microphone. On the measurement grid, nine measurement points are located, each of them having horizontal and vertical distance from the neighboring points on the same alignment s of 0.40 m (see Fig. 3). The microphone is subsequently placed in each of the nine measurement points, at a horizontal distance d_M of 0.25 m from the microphone plane of reference, and an impulse response is sampled in each measurement point. When the microphone is in the central position of the measurement grid, the acoustic center of the sound source and the acoustic center of the microphone must lie on the same line normal to the two planes of reference and must have the same height, equal to half the barrier height [Fig. 2(a)].

A free-field measurement is taken displacing the loudspeaker and the microphone far from any nearby object. In particular, the distance of the microphone from the sound source must be kept equal to the distance when the equipment is in the position 5 [see Fig. 2(b)]:

$$d_{\mathrm{TOT}} = d_S + t_B + d_M = 1{,}25 + t_B . \tag{7}$$

The nine measurements taken on the measurement grid plus the corresponding free-field measurement shall be processed and averaged according to the sound insulation index formula, Eq. (3). Figure 8 shows the single results of the nine measurements taken in front of the barrier elements and the final logarithmic average for sample MET1.

For noise barriers constituted by one or several acoustic elements sustained by vertical posts at fixed distances, a set of nine measurements on the measurement grid plus a free-field measurement must be performed both close to the middle of a representative element and facing a representative post. This permits the detection of the two most common kinds of sound leaks, which are usually located at panel–panel and panel–post connections.

If it is suspected that sound leaks may exist at a different position, e.g., at the bottom edge of the barrier under test, a further set of nine measurements on the measurement grid plus a free-field measurement can be performed placing the measuring equipment close to that position. In this particular case, the sound signal coming from the bottom edge is no longer a ''parasitic'' signal: it is of course, the ''transmitted'' signal one is looking for. The *Adrienne* window must then be enlarged so as to include this signal and to avoid other parasitic signals, on the basis of a geometrical computation to be shown on the test report. Among the possible parasitic signals, the ground reflection on the receiver side is not of concern, as the apparent sound source, i.e., the leak, is located on the ground.

Any object other than the device under test shall be considered a reflecting object which could cause parasitic reflections (e.g., safety rails, fences, rocks, parked cars, etc.). These objects must remain far from the microphone.

3. Temporal window

For the *Adrienne* test method, the analysis window must be uniquely defined in shape, length, and position. The analysis window must be the new *Adrienne* window, described in Refs. 7 and 10. It is a composite analysis window, built as follows (see also Fig. 5):

(i) a leading edge having a left-half Blackman-Harris shape and a total length of 0.5 ms;
(ii) a flat portion having a total length of 5.18 ms (main body); and
(iii) a trailing edge having a right-half Blackman-Harris shape and a total length of 2.22 ms.

The total length of the *Adrienne* window is 7.9 ms; if the window length has to be varied (this occurs only in exceptional cases), the lengths of the flat portion and the right-half

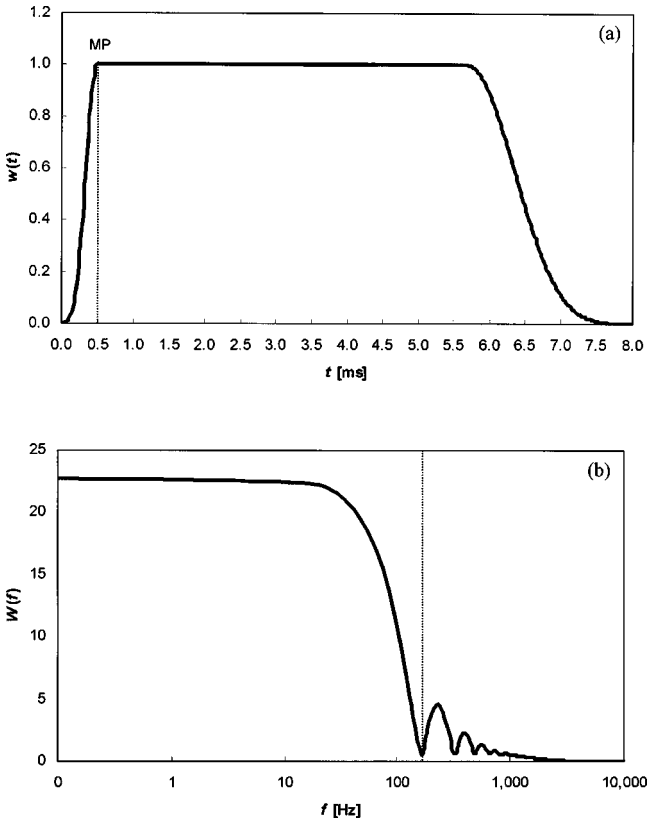

FIG. 5. The *Adrienne* analysis window. (a) In the time domain, the dotted line shows the marker point MP. (b) In the frequency domain (positive frequencies only), the dotted line shows the end of the main lobe.

Blackman-Harris portion must have a ratio of 7/3. The point where the flat portion of the Adrienne window begins is called the marker point (MP).

For the direct ''free-field'' component, the window is placed as follows (Fig. 6):

(i) the maximum peak of the impulse response is detected;
(ii) a time instant preceding the direct component peak of 0.2 ms is located; and
(iii) the *Adrienne* window is placed so as its marker point corresponds to this time instant.

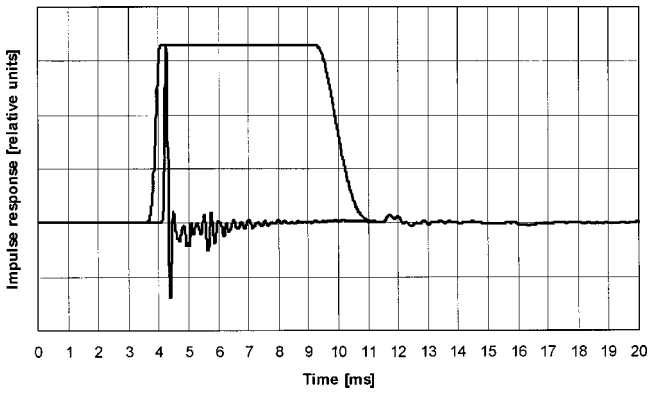

FIG. 6. The *Adrienne* window applied at the free-field component (sample MET1).

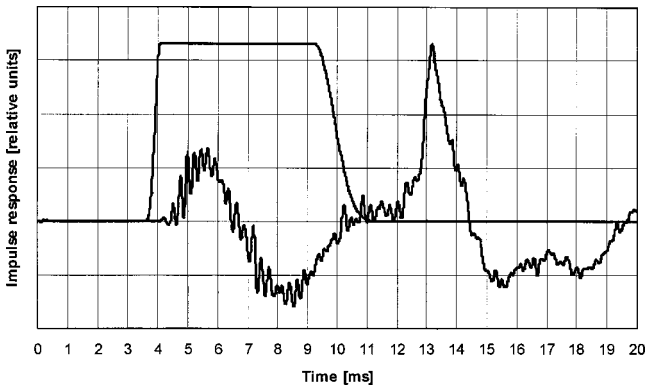

FIG. 7. The *Adrienne* window applied at the transmitted component; position 5 in front of an acoustic element (sample MET1).

In other words, the direct component *Adrienne* window is placed so as its flat portion begins 0.2 ms before the direct component peak.

For the transmitted component, the window shall be placed as follows (Fig. 7):

(i) the time instant when the transmission begins is located, possibly with the help of geometrical computation (conventional beginning of transmission);
(ii) a time instant preceding the conventional beginning of transmission of 0.2 ms is located;
(iii) the transmitted component *Adrienne* window is placed so as its marker point corresponds to this time instant;
(iv) the time instant when the diffraction begins is located, possibly with the help of geometrical computation (conventional beginning of the diffraction); and
(v) the transmitted component *Adrienne* window stops 7.4 ms after the marker point or at the conventional beginning of the diffraction, whichever of the two comes first.

In other words, the transmitted component *Adrienne* window is placed so that its flat portion begins 0.2 ms before the first peak of the transmitted component and its tail stops before the beginning of the diffraction.

Using these rules, the placement of the analysis window can be done automatically, without relying on the operator's skills (actually, the rules are implemented in the program ALFA©, developed by the authors and used for processing the data presented in this article). In computations involving the sound speed *c*, its temperature-dependent value must be assumed.

It is worth noting that the first peak of the direct ''free-field'' component is also the maximum peak. This is not necessarily true for the transmitted component, whose shape depends on the structural and vibrational characteristics of the barrier under test. For example, Fig. 7 shows the impulse response measured at position 5 in front of the panels of the metallic barrier MET1. Geometrical computation confirms that the windowed component is the transmitted one, while the maximum peak coming after it corresponds to the diffraction over the top edge of the screen.

The window length of 7.4 ms after the marker point can

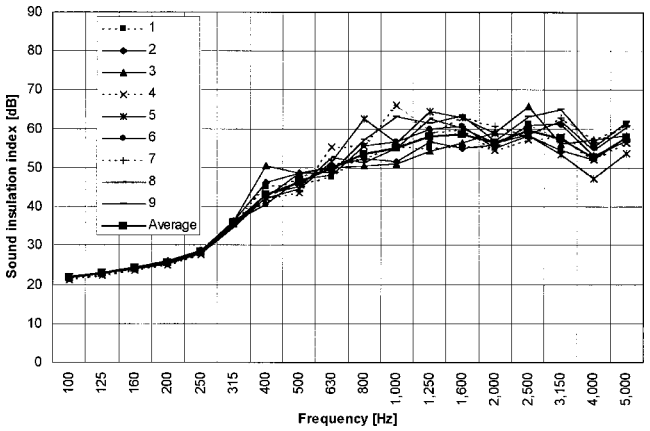

FIG. 8. Sound insulation index values measured at the nine scanning positions in front of the acoustic elements and final logarithmic average (sample MET1).

be explained with an example, assuming for the sake of simplicity an infinitely thin screen ($t_B \approx 0$) with a height h_B of 4 m. Let d_{SE} be the distance between the loudspeaker and the diffracting to edge and d_{EM} the distance between the diffracting top edge and the microphone in the central top position, position 2 (Figs. 9 and 3). The minimum path length of the diffracted signal is

$$d_{SEM} = d_{SE} + d_{EM} = \sqrt{d_S^2 + \left(\frac{h_B}{2}\right)^2} + \sqrt{d_M^2 + \left(\frac{h_B}{2} - s\right)^2} = 3.86 \ \text{(m)}, \tag{8}$$

where h_B is the barrier height. The minimum path length of the transmitted signal is

$$d_{SM} = \sqrt{(d_S + d_M)^2 + s^2} = 1.31 \ \text{(m)}. \tag{9}$$

The time delay gap corresponding to the path length difference between the transmitted and diffracted signals therefore is

$$\tau = \frac{d_{SEM} - d_{SM}}{c} = 7.4 \ \text{(ms)}, \tag{10}$$

exactly the *Adrienne* window length, apart from the ''prewindow'' (left Blackman-Harris edge of 0.5 ms).

4. Low-frequency limit

The low-frequency limit of sound insulation index measurements is inversely proportional to the width of the analysis window and depends also on its shape; taking the first notch in the magnitude spectrum of the window as an indicator of the low-frequency limit,[27,28] for an *Adrienne* window 7.9 ms wide, this limit is about 160 Hz [see Fig. 5(b)].[29] It can be reduced increasing the window width, which is possible when the height of the noise barrier under test is greater than 4 m. Strictly speaking, the outdoor measured values shown in the following for 4-m-tall barriers are therefore valid only starting from the 200-Hz one-third octave band. In spite of this, on the graphs (Figs. 10–17) also the values measured in the 100- to 160-Hz one-third octave bands have been retained, just to have an idea of their consistency with laboratory results. The correlations between outdoor and laboratory results presented in Sec. V have of course been obtained on the valid frequency range 200 Hz to 5 kHz.

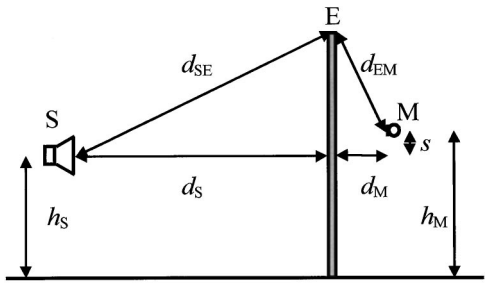

FIG. 9. For the computation of the *Adrienne* window length (see text).

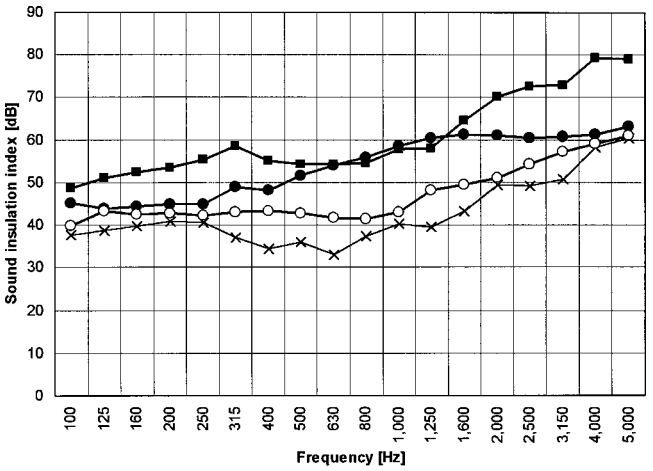

FIG. 10. Sound insulation index values for barrier CON2: (●) laboratory measurements—accurate seal; (○) laboratory measurements—quick seal; (■) outdoor measurements—elements; (×) outdoor measurements—post.

IV. OUTDOOR MEASUREMENTS

A. Measuring equipment

The measurement system was assembled using the following devices:

(1) Sound source: prototype diffusor built inserting a single loudspeaker driver (JBL type 2123H, diameter 250 mm) in a closed cabinet with parallelepiped shape.
(2) Loudspeaker amplifier: QSC USA 1300.
(3) Parametric equalizer: BSS Audio FCS-926 ''varicurve'' with 12 parametric filters.
(4) Microphone Brüel & Kjær type 4190, with Brüel & Kjær type 2669 preamplifier and Brüel & Kjær type 2807 power supply.
(5) Sampling digitizer board: A2D-160 board, containing the MLS generator, the programmable eight-pole antialiasing filter and the A/D converter (having an effective resolution of 16 bits).
(6) Toshiba T6600C portable computer, containing the A2D-160 board.

The A2D-160 board is driven by the MLSSA© software[30] for the generation of the MLS signal and the acquisition of the impulse response; the rest of the signal processing is done using ALFA©, a special-purpose software developed by the authors. The test signal was a MLS sequence of order 16

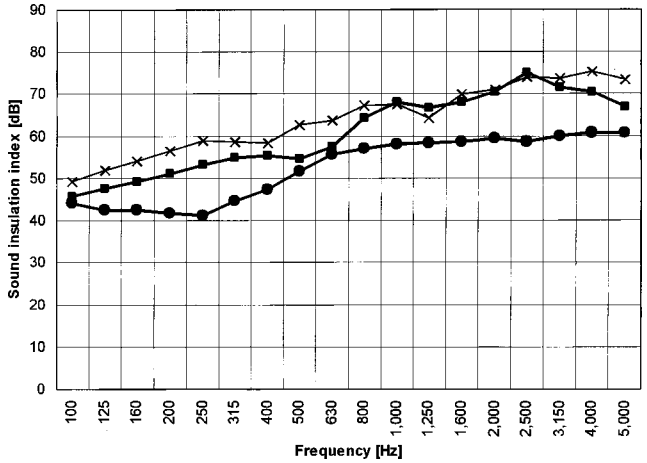

FIG. 11. Sound insulation index values for barrier CON4: (●) laboratory measurements; (■) outdoor measurements—elements; (×) outdoor measurements—post.

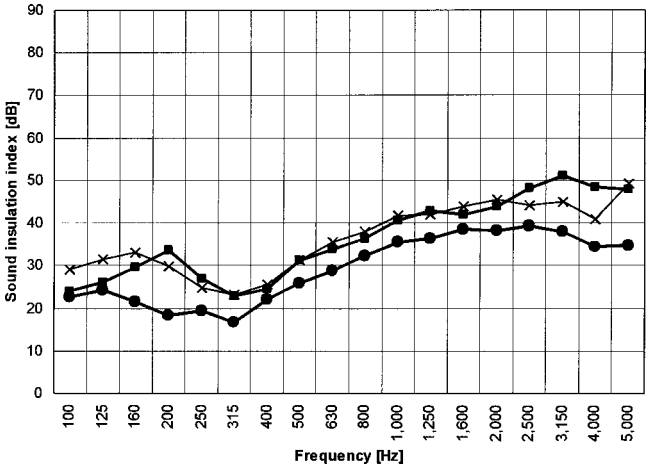

FIG. 14. Sound insulation index values for barrier MET5: (●) laboratory measurements; (■) outdoor measurements—elements; (×) outdoor measurements—post.

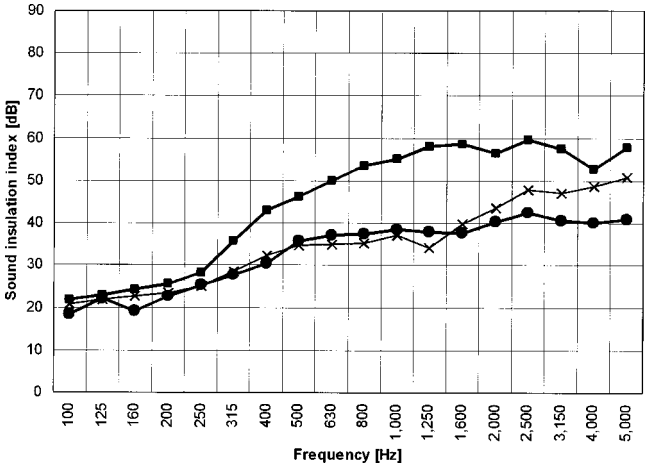

FIG. 12. Sound insulation index values for barrier MET1: (●) laboratory measurements; (■) outdoor measurements—elements; (×) outdoor measurements—post.

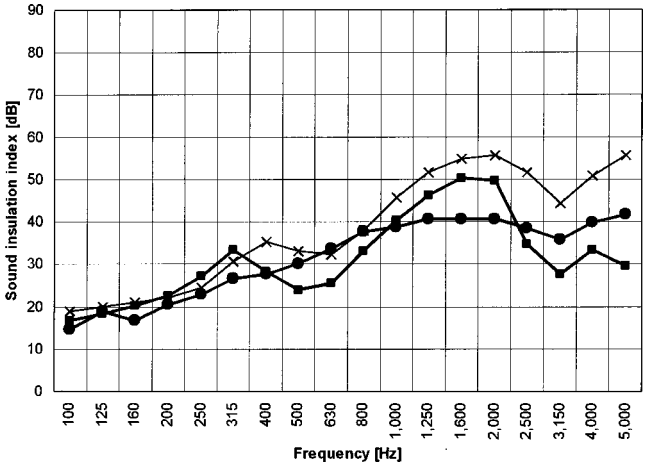

FIG. 15. Sound insulation index values for barrier MET6: (●) laboratory measurements; (■) outdoor measurements—elements; (×) outdoor measurements—post.

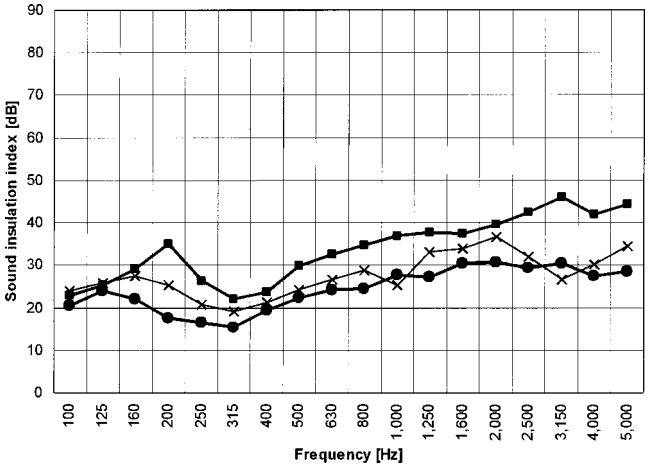

FIG. 13. Sound insulation index values for barrier MET4: (●) laboratory measurements; (■) outdoor measurements—elements; (×) outdoor measurements—post.

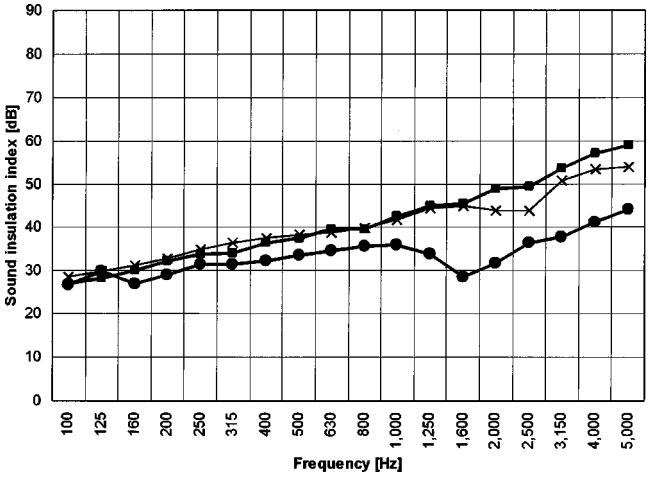

FIG. 16. Sound insulation index values for barrier ACR1: (●) laboratory measurements; (■) outdoor measurements—elements; (×) outdoor measurements—post.

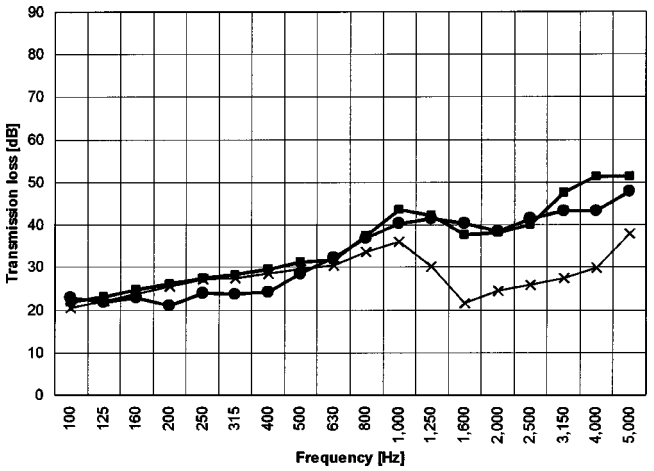

FIG. 17. Sound insulation index values for barrier WOOD: (●) laboratory measurements; (■) outdoor measurements—elements; (×) outdoor measurements—post.

generated by the A2D-160 board;[30] 64 averages were performed for each impulse response acquisition.

B. Outdoor test site

The test site is a flat, grass-covered ground. The grass was cut before the beginning of the tests. No trees, stones, or other reflecting objects were present in a $50\times 50\,\mathrm{m}^2$ area around the noise barrier under test. All samples were built in the same place and removed after the test, one after the other. Measurements were taken in good meteorological conditions, with no rain or strong wind (wind speed always <4 m/s).

Background noise was very limited, the only noise source being a local road, where few cars pass every day, 50 m away from the test samples. Moreover, it is well known that MLS technique is strongly noise rejecting.[19,21,23] In any case, when some occasional noise occurred, like airplane flyovers, measurements were repeated and it was verified that the extraneous noise had no influence.

C. Outdoor measurement results

Examples of outdoors measurements are reported in graphical form in Figs. 10–17 together with the corresponding laboratory measurements (see Sec. II). In each graph, three curves are shown, because, as stated in Sec. III D 2, for each noise barrier the outdoor measurement procedure was repeated two times, placing the measuring equipment first close to the acoustic elements and then close to a representative post. This permitted the investigation of the two most common kinds of sound leak, which are usually located at panel–panel and panel–post connections.

For each barrier sample tested outdoors, the single number rating DL_{SI} was computed, using the formula (2) with SI_j in place of R_j. Due to the above-mentioned low-frequency limit of outdoor measurements (see Sec. III D 4), the calculations were performed in the one-third frequency bands from 200 Hz to 5 kHz. The results are reported in Table III.

V. COMPARISON BETWEEN LABORATORY AND OUTDOOR DATA

There is a general tendency for the laboratory results to be lower than the outdoors results for the same kind of barrier. This may be due to the different sound fields in front of the test specimen: diffuse field in laboratory, frontal free-field outdoors. In fact, the oblique components of the diffuse field generate the coincidence effect, which of course is not possible outdoors. This is particularly clear in Fig. 16 for sample ACR1, constituted by a simple homogeneous acrylic sheet: the laboratory curve exhibits an evident coincidence dip in the 1600-Hz one-third octave band; for outdoors measurements this effect is absent. Moreover, the steady-state signal recorded in the laboratory is very different from the impulse response recorded outdoors (Raes[13] distinguished between ''static'' and ''dynamic'' transmission loss). Finally, the boundary conditions for the laboratory and the outdoors test samples are very different: rigidly clamped on four sides in the laboratory, relatively free on three sides outdoors. Therefore, differences between laboratory and outdoor values were expected. Actually, one of the aims of this work was to find a correlation between airborne sound insulation values measured using the laboratory and *Adrienne* procedures (see later in this article).

In most cases, sound insulation index values measured outdoor in front of a post are worse than values measured in front of the acoustic elements, especially at high frequency (see, for example, Figs. 10, 12, and 13). This happens when the connections between the acoustic elements and the posts are not perfect and may depend not only on the workmanship, but also on the design of connections and the lack of good seals. In these cases, the laboratory performance is influenced by the element/post connections and is closer to the outdoor performance in front of a post. This confirms the importance of including a post in the test, both in laboratory and outdoors. For the concrete barrier CON2 (Fig. 10), the laboratory test was repeated two times, the first with a

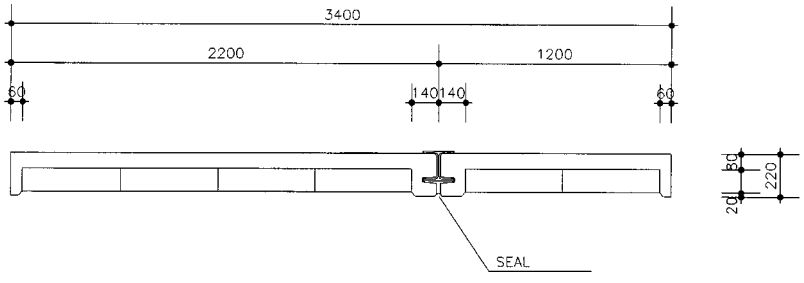

FIG. 18. Barrier CON4: plan view of typical components. Dimensions in millimeters.

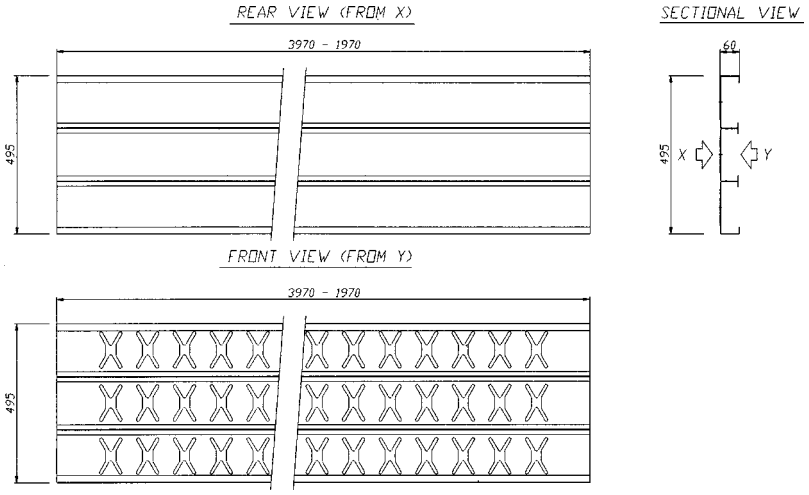

FIG. 19. Barrier MET4: front, rear, and sectional view of the sample for outdoor measurements. Dimensions in millimeters.

''quick'' seal at posts—similar to those used outdoors—and the second with an accurate seal. As can be seen, with the quick seal the laboratory performance is closer to the outdoor performance measured in front of a post, while with the accurate seal the laboratory performance is closer to the outdoor performance in front of barrier panels. The two different cases are indicated in Table III with CON2(Q) and CON2(A), respectively.

The concrete barrier CON4 gives an apparently anomalous result: the post performance is better than the element performance, and both are better than the laboratory result (Fig. 11). This can be easily explained looking at the barrier structure: posts are divided in two halves, each one being a massive concrete beam, 220 mm thick; each half-post forms a single block with the back panel of a barrier element, 80 mm thick, which supports light clay aggregate blocks, 120 mm thick (Fig. 18). The blocks contain cavities connected to front holes on the exposed face and are intended to act as resonators to improve the sound absorption. Connections are formed between half-posts, blocking them on a steel beam and adding a further seal. From this design, one can expect a better outdoor performance close to posts. In the laboratory, the use of a diffuse sound field results in lower airborne sound insulation values.

The sample MET1 (Fig. 12) is a metallic barrier with evident problems of connections between elements and posts; outdoor the difference is remarkable (6 dB in DL_{SI} values); in the laboratory the result is strongly conditioned by the presence of the post.

The samples MET4 and MET5 (Figs. 13 and 14) are actually the same barrier: MET4 is constituted of 1.0-mm metallic sheets, folded to form protruding supports, 60 mm wide (Fig. 19). MET5 is MET4 plus a lining in polyester fiber wool panels (see Table I). For barrier MET5 all joints were carefully sealed. With the additional treatment the overall performance is better (in terms of single number rating, 3-dB gain in the laboratory and 6-dB gain outdoors close to posts; see Table III); for barrier MET5 the single number rating DL_{SI} obtained close to a post is equal to that obtained close to metallic panels.

For the sample MET6 (Fig. 15) the metallic sheets are relatively free to vibrate. This conditions the outdoor performance: the sound insulation index is better close to posts, made with a rigid steel beam. In the laboratory, where the test specimen is clamped on four sides, the mobility is reduced and the sound transmission can be influenced.

For the barrier WOOD, the low values at high frequency of the sound insulation index measured outdoors close to a post (Fig. 17) are due to an evident leakage at panel–post connection, detectable by visual inspection.

Comparing the values reported in Table III with the categories shown in Table II, it is worth noting that all samples, excluding MET4 (laboratory test) and RES1 (laboratory test 100 Hz to 5 kHz and outdoor post test), got a category B3 of airborne sound insulation, according to EN 1793-2; the present EN classification does not allow discrimination among barriers with a single number rating greater than 24 dB.

Looking at Figs. 10–17, it can also be noticed that outdoor measured values in the one-third octave frequency bands from 100 to 160 Hz, while outside the range of validity as discussed in Sec. III D 4, are consistent with the laboratory measured values.

The application of standard statistical theory to data of Table III permitted us to obtain linear correlation laws be-

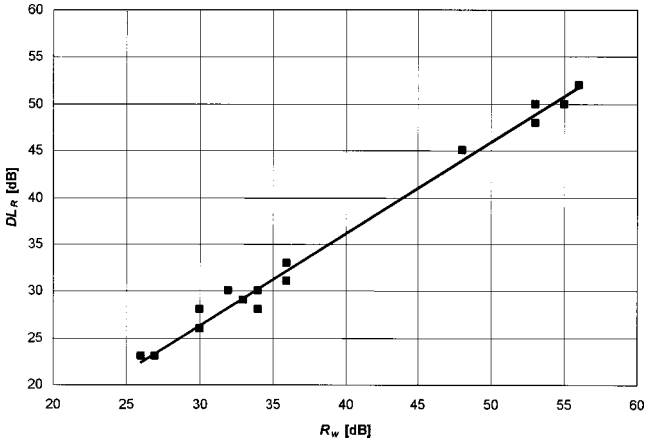

FIG. 20. Linear correlation between the single number ratings R_w and DL_R obtained from laboratory data. Frequency range: one-third octave bands from 100 Hz to 5 kHz.

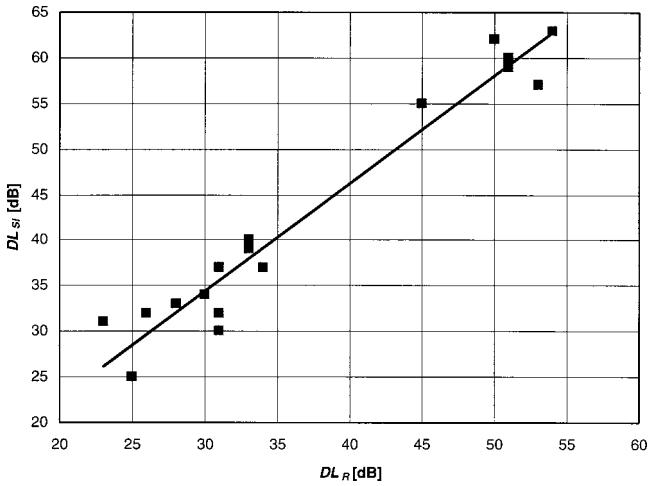

FIG. 21. Linear correlation between the single number ratings obtained in laboratory (DL_R) and outdoors in front of the barrier acoustic elements (DL_{SI}). Frequency range: one-third octave bands from 200 Hz to 5 kHz.

tween airborne sound insulation rating figures obtained using the laboratory and *Adrienne* procedures.

Figure 20 shows the correlation between the values of the two single number ratings obtained from laboratory measurements, calculated over the frequency range 100 Hz to 5 kHz, the DL_R specified in EN 1793-2 and the R_w specified in ISO 717-1:[11]

$$DL_R = 0.98R_w - 3.05 \quad (r = 0.995). \tag{11}$$

Using the same values of R_w and the values of DL_R calculated over the frequency range 200 Hz to 5 kHz, the correlation becomes

$$DL_R = 0.93R_w + 0.37 \quad (r = 0.992). \tag{12}$$

The controlled conditions of the tests and the excellent value of the correlation coefficient r support the conclusion that on average the EN single number rating DL_R is few decibels lower than the index R_w used in building acoustics.

Figures 21 and 22 show the linear correlation laws between the single number rating DL_R obtained from laboratory data and the single number rating DL_{SI} obtained from outdoor data measured close to barrier elements and to posts, respectively. All ratings are calculated over the frequency range 200 Hz to 5 kHz. For barrier CON2, submitted as previously explained to two laboratory tests with different seals at posts, the ''quick'' seal rating (44 dB) was taken for the correlation with the outdoor ratings of measurements close to a post and the accurate seal rating (53 dB) was taken for the correlation with the outdoor ratings of measurements close to the acoustic elements:

$$\text{Elements: } DL_{SI} = 1.18DL_R - 0.94 \quad (r = 0.97), \tag{13}$$

$$\text{Posts: } DL_{SI} = 1.18DL_R - 3.16 \quad (r = 0.93). \tag{14}$$

The linear correlation coefficient r is excellent for elements and very good for posts; this difference was expected, because outdoor results are less regular at posts due to the above-mentioned problems of panel–post connections. In any case, the high values of the correlation coefficient support the conclusion that Eqs. (13) and (14) can be useful for predicting the expected field performance from laboratory data measured according to EN 1793-2.

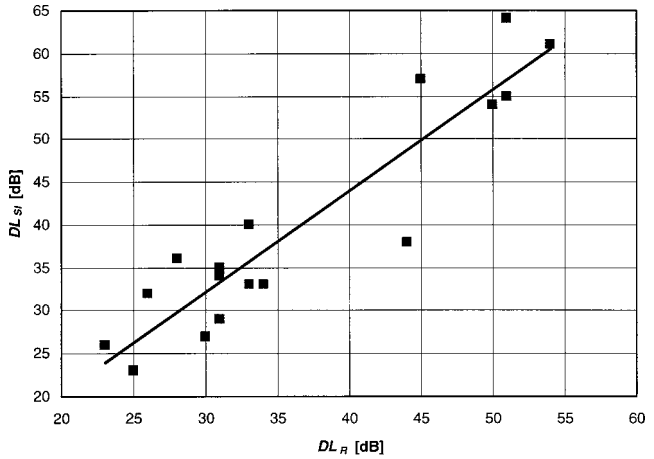

FIG. 22. Linear correlation between the single number ratings obtained in laboratory (DL_R) and outdoors in front of barrier posts (DL_{SI}). Frequency range: one-third octave bands from 200 Hz to 5 kHz.

VI. CONCLUSIONS

A detailed verification of the *Adrienne* test method for airborne sound insulation over a selection of 17 noise barriers, representative of the Italian and European production, has been done. The new method proved to be easy to use and reliable for all kinds of barrier. It has been found sensitive to quality of mounting, presence of seals, and other details typical of outdoor installations. The comparison between field and laboratory results shows a very good correlation, while existing differences can be explained with the different sound fields and mounting conditions between the outdoor and laboratory tests. In other words, results obtained using the *Adrienne* test method are consistent with laboratory results obtained using EN 1793-2. The correlation laws resulting from the present work can be useful for predicting the airborne sound insulation performance of noise barriers in the field from laboratory data. It can be concluded that the *Adrienne* method is adequate for its intended use.

ACKNOWLEDGMENTS

The measurements reported in this work were done in 1999 by the authors for *Italferr*, the engineering company of *Ferrovie dello Stato* (Italian Railways) responsible for the technical supervision of the Italian high speed railway network. The laboratory tests were performed in the facilities of *Istituto Giordano* (Bellaria, Italy), in the frame of a contract with *DIENCA*. In particular, the authors of this article would like to thank Andrea Bruschi for his invaluable help during laboratory measurements. The outdoor test method used during this work was developed in the frame of the European project *Adrienne*, funded by the European Commission (Contract No. MAT1-CT94049). The main partners of the research were *Acoustical Technologies* (B), *Fraunhofer Institut für Bauphysik* (D), *ENTPE-LASH* (F), and *DIENCA* (I). Other associated partners were *CSTB* (F), *LCPC* (F), *IA-CSIC* (E), *FIGE* (D), and *CEDIA* (B).

[1] I-INCE Publication 98-1, ''Technical assessment of the effectiveness of noise walls,'' Noise/News International **6**, 11–35 (1998).
[2] EN 1793-1, ''Road traffic noise reducing devices—Test methods for determining the acoustic performance—Part 1: Intrinsic characteristics of sound absorption'' (1997). (Information on how CEN Standards can be obtained is available on the Web site http://www.cenorm.be)
[3] EN 1793-2, ''Road traffic noise reducing devices—Test methods for determining the acoustic performance—Part 2: Intrinsic characteristics of airborne sound insulation'' (1997). (Information on how CEN Standards can be obtained is available on the Web site http://www.cenorm.be)
[4] EN 1793-3, ''Road traffic noise reducing devices—Test methods for determining the acoustic performance—Part 3: Normalized traffic noise spectrum'' (1997). (Information on how CEN Standards can be obtained is available on the Web site http://www.cenorm.be)
[5] ISO 354, ''Acoustics—Measurement of sound absorption in a reverberation room'' (1985).
[6] ISO 140-3, ''Acoustics—Measurements of sound insulation in buildings and of buildings elements. Part 3: laboratory measurements of airborne sound insulation of building elements'' (1995).
[7] *Adrienne* Research Team, ''Test methods for the acoustic performance of road traffic noise reducing devices—Final report,'' European Commission, DGXII SMT Project MAT1-CT94049 (1998).
[8] AFNOR S 31-089, ''Code d'essai pour la détermination de caractéristiques acoustiques d'écrans installés en champ libre'' (1990).
[9] J.-P. Clairbois, J. Beaumont, M. Garai, and G. Schupp, ''A new *in-situ* method for the acoustic performance of road traffic noise reducing devices,'' J. Acoust. Soc. Am. **103**, 2801(A) (1998).
[10] F. Anfosso, M. Garai, and J-P. Clairbois, ''*Adrienne*: une méthode européenne pour la qualification sur site des écrans antibruit,'' Bullettin des Laboratoires des Ponts et Chausées, n. 225, 89–104 (2000).
[11] ISO 717-1, ''Acoustics—Rating of sound insulation in buildings and of buildings elements. Part 1: airborne sound insulation'' (1996).
[12] A. C. Raes, ''A tentative method for the measurement of sound transmission losses in unfinished buildings,'' J. Acoust. Soc. Am. **27**, 98–102 (1955).
[13] A. C. Raes, ''Static and dynamic transmission losses of partitions,'' J. Acoust. Soc. Am. **35**, 1178–1182 (1963).
[14] P. de Tricaud, ''Impulse techniques for the simplification of insulation measurement between dwellings,'' Appl. Acoust. **8**, 245–256 (1975).
[15] J. Roland, ''Airborne isolation measurements by impulse technique,'' Noise Control Eng. J. **16**, 6–14 (1981).
[16] J. C. Davies and B. M. Gibbs, ''The oblique incidence measurement of transmission loss by an impulse method,'' J. Sound Vib. **74**, 381–393 (1981).
[17] Y. A. Balilah and B. M. Gibbs, ''The measurement of the transmission loss of single leaf walls and panels by an impulse method,'' J. Sound Vib. **123**, 229–245 (1988).
[18] W. Zuomin and W. T. Chu, ''Ensemble average requirement for acoustical measurements in noisy environment using the *m*-sequence correlation technique,'' J. Acoust. Soc. Am. **94**, 1409–1414 (1993).
[19] M. R. Schroeder, ''Integrated impulse method measuring sound decay without impulses,'' J. Acoust. Soc. Am. **66**, 497–500 (1979).
[20] J. Borish and J. B. Angell, ''An efficient algorithm for measuring the impulse response using pseudorandom noise,'' J. Audio Eng. Soc. **31**, 478–488 (1983).
[21] D. D. Rife and J. Vanderkooy, ''Transfer-function measurement with maximum-length sequences,'' J. Audio Eng. Soc. **37**, 419–444 (1989).
[22] J. Vanderkooy, ''Aspects of MLS measuring systems,'' J. Audio Eng. Soc. **42**, 219–231 (1994).
[23] M. Garai, ''Measurement of the sound-absorption coefficient *in situ*: the reflection method using periodic pseudo-random sequences of maximum length,'' Appl. Acoust. **39**, 119–139 (1993).
[24] C. Bleakley and R. Scaife, ''New formulas for predicting the accuracy of acoustical measurements made in noisy environments using the averaged *m*-sequence correlation technique,'' J. Acoust. Soc. Am. **97**, 1329–1332 (1995).
[25] M. Vorländer and M. Kob, ''Practical aspects of MLS measurements in building acoustics,'' Appl. Acoust. **52**, 239–258 (1997).
[26] E. Mommertz, ''Angle-dependent *in-situ* measurements of reflection coefficients using a subtraction technique,'' Appl. Acoust. **46**, 251–263 (1995).
[27] S. Gade and H. Herlufsen, ''Use of weighting functions in DFT/FFT analysis (Part I),'' Brüel & Kjær Technical Review no. 3 (1987), pp. 1–28.
[28] S. Gade and H. Herlufsen, ''Use of weighting functions in DFT/FFT analysis (Part II),'' Brüel & Kjær Technical Review no. 4 (1987), pp. 1–35.
[29] P. Cobo, ''Some calculations concerning the *Adrienne* setup and the lowest reliable frequency,'' Report to the *Adrienne* Research Team (1998).
[30] D. D. Rife, *MLSSA Reference Manual vr. 10.0A* (DRA Laboratories, Sterling, VA, 1996).